Technical Note

AN EXPERIMENTAL AND THEORETICAL INVESTIGATION OF CORROSION MECHANISM IN A METALLIC STACK

M. R. Sarmasti Emami

* *m_r_emami@iust.ac.ir*

Iran University of Science &Technology, Tehran, Iran.

Abstract: This paper presents an experimental and theoretical investigation of the causes of corrosion of stack in a cement plant. In this paper, information related to metallic stack failures are given in the form of a case study in Neka Cement Plant, Mazandaran, Iran. Heavy corrosion attacks were observed on the samples of stack. The failure can be caused by one or more modes such as overheating, stress corrosion cracking (SCC), hydrogen embrittlement, creep, flame impingement, sulfide attack, weld attack, dew point corrosion, etc. Theoretical calculations and experimental observations revealed that, the corrosion had taken place due to the condensation of acidic flue gases in the interior of stack. Also, the chemical analysis of the corrosion deposits and condensates confirmed the presence of highly acidic environment consisting of mostly sulfate ions.

1. INTRODUCTION

Corrosion has been the subject of scientific study for more than 150 years. There are three primary reasons for concern about and the study of corrosion-safety, economics, and conservation. Corrosion is defined as an interaction between a metal and its environment that results in changes in the properties of the metal, and which may lead to significant impairment of the function of the metal, the environment, or the technical system, of which these form a part [1]. Corrosion is expensive. At US $2.2 trillion, the annual cost of corrosion worldwide is over 3% of the world's Gross Domestic Product. Yet, governments and industries pay little attention to corrosion except in high-risk areas like aircraft and pipelines [2]. The two-year study estimated that corrosion impacts in the cement plants nearly $276 Billion [3]. The specific mechanism of the corrosion process at the metal surface/environment interface and the controlling factory vary from case to case and are highly complex. However, all metallic corrosion is electrochemical and involves the operation of what is described as a "corrosion cell" (Fig. 1).

For a corrosion cell to operate, the following four conditions must be satisfied: a- The surface of the structure must have both anodic and cathodic areas, b- The anodes and cathodes must be immersed in a continuous ionized electrolyte,

c- The anodes and cathodes must be electrically connected through a metallic path and d- There must be an electrical potential between the anodes and cathodes.

When these conditions exist, a corrosion cell is formed in which an electric current flows from the anode to the cathode through the electrolyte. Depending on the specific conditions, the physical size of the corrosion cell can vary from very small (within a single drop of moisture on a metal-surface transmission pipeline) to very large. Metal loss occurs at the anode, while the surface is protected from corrosion damage at the cathode. The amount of metal lost at the anode is
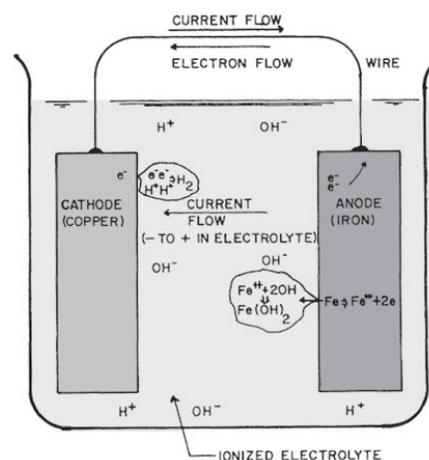

Fig. 1. Schematic diagram of a iron/copper corrosion cell

directly proportional to the corrosion cell current flow in amperes. Depending on the specific physical and metallurgical nature of each metal and the prevailing environmental conditions, different types of corrosion activity will occur. Although they appear to be different in the final form of damage, all are examples of this fundamental corrosion cell.

As one can see from this fundamental discussion, the determinations of the causes of corrosion in a specific case are extremely complex. There are many variables, many of which are dynamic, that complicate the matter. This article describes the failure analysis that has been carried out to ascertain the cause of accelerated corrosion and failure of material used in a stack in a cement plant.

2. THEORETICAL PROCEDURE

The following parameters were determined in the stack flue gases by Environment Protection Agency of Iran: SO_3, SO_2, NOx, CO, CO_2, O_2, hydrocarbons. Flue gas temperature was monitored using a portable flue gas analyzer (TESTO-350 XL). Molar fraction of stack flue gas is given in the table 1. Results of table 1 were

Table 1. mole fraction of flue gases of the stack

Component	Mole fraction
CO_2	0.2414
CO	0.000017
N_2	0.45
NO	0.000188
NO_2	0.0000038
SO_2	0.0007852
SO3	0.0000413
O_2	0.021511
H_2O	0.2733
Unburned Hydrocarbon	0.0000249

used for determining the dew point temperature and pH calculations of flue gases in stack of Neka cement plant.

2. 1. Calculation of Dew Point Temperature

When fuel oil is burned in any combustion process, the sulfur oxides and combines with the process gas moisture to form sulfuric acid. Although the chemistry is simple, predicting where acid may condense in a system is difficult. The most practical solution is to measure the acid dew point temperature. Two simple formulations that allow calculation of temperature, pressure and phase compositions for vapor/liquid systems are Raoult's Law and Henery's Law. These two laws have achieved on the basis two essential assumptions. First, vapor phase is ideal gas and that the second liquid activity coefficient is equal to the unit [4]. Because sulfur trioxide have high solubility in water, then Raoult law is used for it. For other component, because limited solubility is existed, therefore Henrry law is used.

$$Y_iP = X_iH_i \qquad i = CO_2, CO, NO, NO_2, O_2, SO_2, N_2 \qquad (1)$$

$$Y_jP = X_jP_j(saturate) \qquad j = SO_3 , H_2O \qquad (2)$$

$$(X_i+Y_j) = P/ (H_i/Y_i+P_j/Y_j) \qquad (3)$$

$$P (calculate) = 1/ (Y_i/H_i +Y_j/P_j) \qquad (4)$$

Inlet and outlet pressure of flue gas flow in the stack were 0.909 and 1 atmosphere respectively. If try and error method is used, dew point temperatures in the inlet and outlet stack are determined 65.2 and 67.45 °C respectively. It should be mentioned that the dew point of flue gases containing sulfuric acid significantly increased [5]. The temperature of flue gases in the stack is lower than the boiling temperature of sulfuric acid, so it cannot exist in vapor phase. Although, it exist the tendency among a lot of SO_3 and H_2O in the vapor phase, as a result fine droplets containing acid (acid mist) can be formed. With regard to convection and radiation heat transfer on the external of surface of the stack, following values for internal temperature surface of the stack can be achieved [6].

Fig. 2. corrosion products in the interior surface of stack

Therefore, it can be found even without the possibility of increasing the dew point temperature, in the 23 m top of stack, internal surface temperature will fall to dew point temperature. As a result, a liquid film on the internal surface is formed. Even if the condensation is not continuous, the effect of corrosion is accumulative. As the thickness of the rust layer increases, eventually corrosion flakes disbond from the metal surface and the flue gases push them out. This is often visible in the neighborhood of a corroding stack. Figure 2 shows these rust scales inside a stack.

2. 2. Determination of pH

According to calculations performed it was found that a liquid film on the inner surface of the stack is formed. Now determine the combustion gases solubility in the pH level of the film we get an approximate basis. According to calculations performed it was found that a liquid film on the inner surface of the stack is formed. Now determine the combustion gases solubility in the pH level of the film we get an approximate basis. The only acid that can effectively process corrosion company to sulfuric acid because other compounds such as CO_2, CO, SO_2 and NO_2, or having solubility limit in water are, or that if absorbed the same amount of limiting in solutions of water and formation of acid related Rate are very low resolution.

With the placement of each mole fraction composition in the dew point temperature liquid phase is given in the table 3.

Basis: 1 mol of solution
$X (SO_3) = N (SO_3) = 1.4714 \times 10^{-5}$
$V (solution) = 0.018$ Lit (1 mol of solution)
$Cm = N (SO_3) / V$ solution
$Cm = 8.212 \times 10^{-4}$ molar

Table 3. Mole fraction in the condensate film

Composition	Mole fraction
N_2	3.4362×10^{-6}
O_2	2.8387×10^{-7}
SO_2	1.58×10^{-5}
CO_2	1.353×10^{-4}
SO_3	1.4714×10^{-5}
H_2O	0.9979

Table 2. Variations of internal surface temperature of stack respect to height and air temperature

	73 m height stack	50 m height stack
(°C) Air temperature	internal surface temperature	internal surface temperature
27	57.6	60.1
10	52.8	55.4
0	49.9	52.6

Because all the sulfur trioxide is absorbed and the formation of sulfuric acid gives the acid to the aqueous environment can be fully ionized, we will:

$$H_2O(l) + SO_3 \Rightarrow H_2SO_4(l) \tag{5}$$

$$H_2SO_4(l) + H_2O(l) \Rightarrow H_3O^+ + HSO_4^- \tag{6}$$
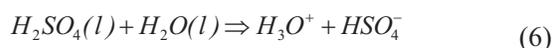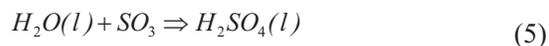
Considering the above relations with molarity H_3O^+ and SO_3 will be equal, so:

$$pH = -log(H_3O^+) \tag{7}$$

According to the above trend, acidity of condensation film (pH) at inlet and outlet of the stack are determined 3.08 and 3.09 respectively.

3. EXPERIMENTAL PROCEDURE

The corrosion experiments and measurements presented in this paper were carried out in a 3.35 m internal diameter 70 m long stack in Neka cement plant. In order to study the corrosion phenomenon of the Stack, a series of measurements and experiments were performed. These results are presented in the following sections.

3. 1. Fuel Oil Analysis

Fuel oil used during the study were withdrawn from the storage tanks and given for analysis to external agencies (Table 4).

Table 4. Major constituents in fuel oil

No.	Parameters	Range
1	Specific Gravity (110 ˚C)	0.87
2	Net Calorific Value (Cal/gr)	9670-9700
3	Sulfur (wt. %)	2.4-2.7
4	Carbon Residue (wt. %)	84-86
5	Hydrogen (wt. %)	12-14
6	Water Content (wt. %)	0.55-0.67

3. 2. Thickness Measurements

In many cases the corrosion effects is dramatic. After 8 years, there is significant wall thickness loss and the stack becomes structurally unsafe. Tables 5 illustrate a case where the top of the stack fell down.

3. 3. Chemical Analysis of Stack Material

After cleaning the cement compositions and corrosion products from the surfaces of samples, those were investigated. It showed that the material used was low-carbon steel containing minor amounts of copper. The amount of copper, carbon, silicon and sulfur in samples were 0.023%, 0.15%, 0.1% and 0.2% respectively.

3. 4. Determination of Hardness

After cleaning and polishing the samples and metallurgical Mount, the hardness of plate is determined. The hardness measurement is carried out on an apparatus of Zwick Company. The head is made of diamond. Several impressions are

Table 5. Thickness measurement before/after corrosion stack

Height (m)	Initial Thickness (mm)	Thickness status (mm)
0 -18.6	12	10-10.2 -10.5
18.6 -52	10	9.9-9.5 -9.2
52 -57	10	7.5-5.1 -5 -4
57 -73	8	Perfectly pierced

made on the plate are measured under microscope. The average of values measured for samples of stacks is 161 Vickers.

3. 5. Evaluation of surface samples with stereo microscope

Initial microscopic viewing should be done utilizing a stereomicroscope, which reveals a three-dimensional scanning of the specimen surface. Surface of samples were studied by stereo microscope. Observations are shown in the figure of 3 to 5. In figure 3 the exterior surface of stack is shown. A main part of the surface is covered with white crystalline deposits. In this section, orange and black sediments are seen to a lower extent.

The sediments in the interior surface of stack are shown in figures 4 and 5. In this section, the sediments are cracked and there is no effect of sediment white crystals. Orange and black corroded sections are observed clearly.

3. 6. Metallography

Metallography consists of the study of the constitution and structure of metals and alloys. Much can be learned through specimen examination with the naked eye, but more refined techniques require magnification and preparation of the material's surface. Optical microscopy is sufficient for general purpose examination; advanced examination and research laboratories often contain electron microscopes (SEM and
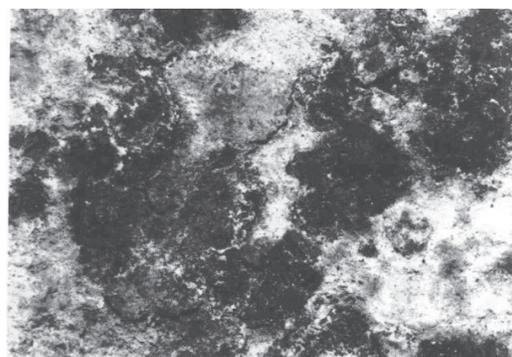

Fig. 4. The stereo image of the interior surface of stack (x 92)

TEM), x-ray and electron diffractometers and possibly other scanning devices.

After cleaning, polishing and mounting, samples were etched by the 2% Nital solution. Nital is a solution of alcohol and nitric acid commonly used for routine etching of metals. It is especially suitable for revealing the microstructure of carbon steels. The microscopic structure of the stack plate is shown in figure 6. Structure of samples is ferrite-perlite and perlite areas are focused in the grain boundary. Therefore, structure of low carbon steels is observed.

3. 7. SEM Observations

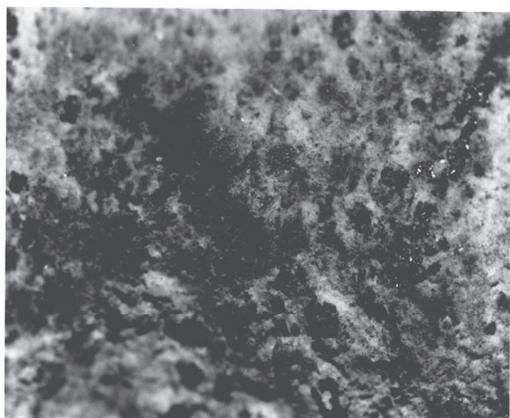Scanning Electron Microscopes (SEMs) are

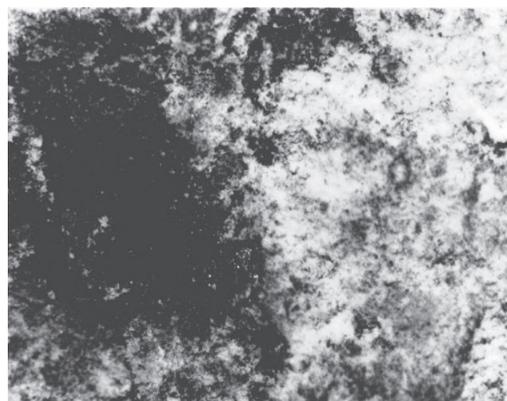**Fig. 3.** The stereo image of the exterior surface of stack

Fig. 5. The stereo image of the interior surface of stack (x 259)

M. R. Sarmasti Emami

capable of magnifications up to 20,000X. SEMs were taken and observed in order to support our findings. Samples of each sample to a square centimeter dimensions obtained by electron microscopy and their surface without applying coating was investigated. SEM images on the flue surface are shown at figure 7 and 8. The pitting and corroded white sediments areas are seen clearly.

3. 8. Chemical Analysis of Corrosion Products

A number of corrosion deposit and/or the condensate samples were collected from different sections of the stack. These samples were analyzed using wet chemical analysis for the presence of anions. In addition to high sulfate content, the condensate/corrosion deposits also contained chloride ions. The pH of the liquid condensate was calculated to be 3. This liquid is formed at the top sections of the stack due to condensation and is collected at the bottom of the stack. The results indicate that the condensate were highly acidic in nature and consisted of mostly H_2SO_4. The above results reflect that the stack materials were exposed to a highly aggressive environment during the operation of the rotary kiln in Neka cement plant.

4. RESULTS AND DISCUSSIONS
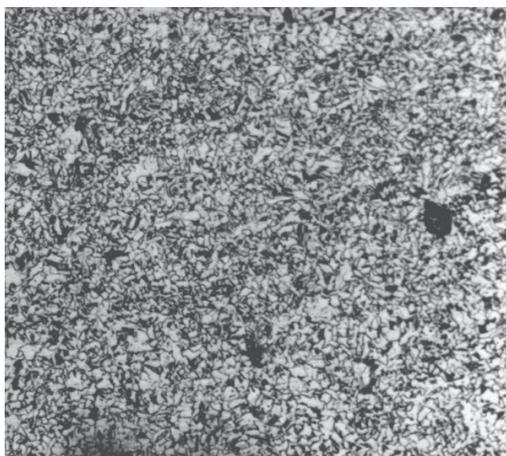
The discussion of the theoretical and experimental results is presented in three sections: (1) the role of sediment composition of cement on corrosion rate, (2) the rule of SO_3 in corrosion phenomena and (3) determination of corrosion rate.

4. 1. Sediment composition

According to the literature, the presence of a rust layer can significantly influence the steel corrosion rate [7–10]. There are two types of deposits on parts corroded are detected. As it mentioned that the above sections, rusting of stack material was studied by means of X-ray and scanning electron microscopy.
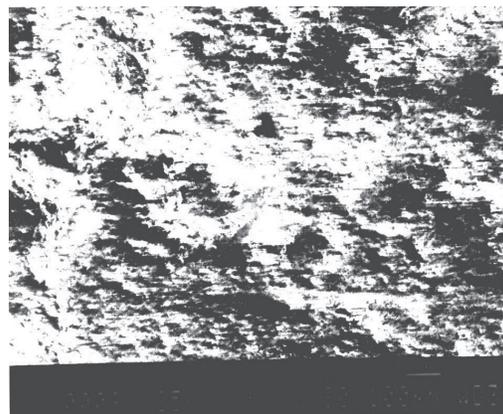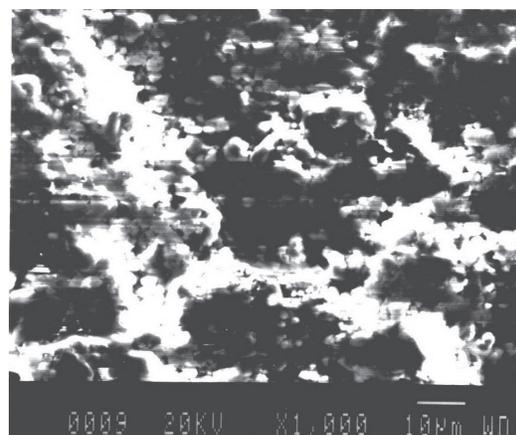

Fig. 7. SEM microscope image surface of stack

Fig. 6. Microscopic structure of stack plate 2% Nital (x 33)

Fig 8. SEM microscope image surface of stack (in higher magnification)

63

A. Cement Deposits

The modern process of cement production involves crushing and grinding of carbonaceous and clayey raw materials under dry conditions, thermal processing of finely ground raw meal, i.e. preheating, precalcining and sintering in rotary kiln, cooling of the clinker (sintered material) on a reciprocating grate cooler and further grinding and packaging of the product cement. Besides this, a great amount of mechanical conveying is also involved. All these operations generate a huge quantity of gas and particulates of varying characteristics, such as temperature, moisture content, particle size distribution, chemical composition, abrassiveness, etc. Chemical compositions of raw materials in Neka cement plant are shown in table 6.

Cement deposits could prevent from reaching the oxygen and any oxidants to the metal surface, but it will be absorption water vapor in flue gases. Thus, always the interior surface of stack has higher moisture than its value in gas phase. As a result, a weak electrochemical cell can be formed in the state.

B. Corrosion Products

If the studied surface is free cement deposits, acidic corrosion effects can be seen obviously. These effects can be seen with naked eye. It was due to oxidants can easier to reach the metal surface. Also, erosion due to flow across the surface disrupts or removes the passive layer. This leaves the exposed metal open to attack from any of the many forms of corrosion [11]. To more accurately assess about the role of these two deposits, we provide two samples of stack material. Samples were subjected into the chloridric acid solution. We observed that the amount of bubbles released in the cement deposits was far less of the cement-free deposits, which represents the cement deposits have strong protection against a corrosive environment.

4. 2. The Rule of SO_3 in Corrosion Phenomena

Fuel oil contains the elements carbon and hydrogen but also a certain amount of sulfur (see table 4). During the combustion process, these elements are rapidly oxidized and the sulfur present in the fuel oil will be combined with oxygen to form sulfur dioxide (SO_2) in a partial oxidation and sulfur

Table 6. Chemical composition of raw materials

Constituent	Analysis, wt%
SiO_2	13.67
Al_2O_3	3.20
Fe_2O_3	2.57
$CaCO_3$	76.91
K_2O	0.33
Na_2O	0.28
$MgCO_3$	3.07

trioxide (SO_3) in a full oxidation, respectively [12]. SO_2 will dissolve in any free moisture that may be present in the flue gas to form sulfurous acid (H_2SO_3). Approximately 1–2% of the SO_2 is further oxidized into SO_3, Which combined with superheated water vapor, forms sulfuric acid vapor (H_2SO_4). Because, the temperature of inside the stack is in the range 90 to 100 ° C, and this temperature range is well below the boiling point of sulfuric acid, therefore it cannot exist in the vapor phase.

The other case is when the temperature of flue gases down to the dew point temperature. In this case, a liquid film is formed on the plates. Due to the high solubility of SO_3, sulfuric acid will be formed into the liquid phase quickly. The amount of SO_3 formed depends on the actual combustion conditions, with the following factors having the greatest influence [13–16]:

- Increase in excess oxygen in combustion.
- Fall in flame temperature.
- Presence of catalysts (V_2O_5, etc.).

Clearly, the greater the mass composition of sulfur in the fuel, the greater the partial pressure of SO_3 will be in the flue gases and, consequently, the temperature for the formation of the acid dew point temperature will rise [17, 18].

4. 3. Determination of Corrosion rate

For final conclusions, we determined the corrosion rate and it compared to the

conventional amounts of steel in atmospheric environments.

Corrosion rate of stack plates = Initial thickness (mm)/ Time (year)

=1.5/8 mm/year= 187.5 µm/year

The average corrosion rate of steel at normal atmospheric temperature was 50 to 130 micrometer per year [19]. Thus, the formations of acids (particularly sulfuric acid) could be main cause accelerate corrosion phenomenon.

5. CONCLUSIONS

In this research, causes of corrosion in the stack of Neka cement plant were investigated experimentally and theoretically. The following results are obtained:

1. Calculations (determining pH and dew point temperature) and experimental confirmation (determine of the corrosion rate, SEM observations and analysis of sediment composition) revealed that acid corrosion is the main causes of corrosion.
2. Erosion is attributable to erosion/corrosion process, but the rule of it was very low respect to acid corrosion.
3. It is well known that carbon steel corrodes rapidly when exposed to the hot, acidic, condensing flue gases produced. Thus it recommended that material of stack is exchanged.

Nomenclature

Cm   Molarity of solution
P_j Saturation pressure
H   Hennery constant
V   Volume of solution
N   Normality
X   Mole fraction in liquid phase
P   Total pressure
Y   Mole fraction in vapor phase

REFERENCES

1. Fontana, M. G., Corrosion engineering, 3 ed., McGraw-Hill Company, USA, 1987, pp. 1-3.
2. http://www.corrosioncost.com/home.html
3. NACE International, News Release, August 15, 2002.
4. Smith, J. M., "Introduction to chemical engineering thermodynamic", 6 ed., McGraw-Hill, Singapore, 1987.
5. Verhoff, F. H., "Predicting dew point of flue gases, Chemical Engineering Progress", 1974, 70, 8.
6. Holman, J. P., "Heat transfer, 6th edition", McGraw Hill, USA, 1986.
7. Evans, R., "Mechanism of rusting, Corrosion Science", 1969, 9, 813.
8. Evans, U. R., Taylor, C. A. J., "Mechanism of atmospheric rusting", Corrosion Science, 1972, 12, 227.
9. Stratmann, M., Bohnenkamp, K., Engell, H. J., "An electrochemical study of phase-transitions in rust layers", Corrosion Science, 1983, 23, 969.
10. Kuch, A., "Invetigations of the reduction and re-oxidation kinetics of iron (III) oxide scales formed in waters", Corrosion Science, 1988, 28, 221.
11. Kruger, J., "Electrochemistry of Corrosion, retrieved February 18", 2009, from Electrochemistry Encyclopedia: http://electrochem.cwru.edu /ed /encycl/art-c02-corrosion.htm.
12. Syri, S., "The impacts of climate change mitigation on air pollutant emissions", in: Technology and Climate Change CLIMTECH 1999–2002; 14/2002 Final Report, The Finnish National Technology Agency, Helsinki, Finland, pp. 224–233, 2002.
13. Beer, J. M., "Combustion technology developments in power generation in response to environmental challenges", Progress Energy Combustion Science, 2000, 26, 301.
14. Peters, N., " Turbulent Combustion, Cambridge University Press", Cambridge, 1998.
15. Koebel, M., Elsener, M., "Thermal optimization of boilers", Chemical Engineering Science, 1998, 53, 6657.
16. Nordin, A., Eriksson, L., Ohman, M., "Comparative analysis of cost of energy", Fuel, 1995, 74, 128, 1995.
17. Hu, Y., Naito, S., Kobayashi, N., Hasatani, M., "CO_2, NOx and SO_2 emissions from the combustion of coal with high oxygen concentration gases", Fuel, 2000, 79, 1925.

18. Nunnari, G., Dorling, S., Schlink, U., Cawley, G., Foxall, R., Chatterton, T., "Modelling SO_2 concentration at a point with statistical approaches", Environ. Model Soft, 2004, 19, 887.

19. NACE Corrosion Engineers Reference Book, NACE publication, Oct. 1983, pp. 72-73.